ADVANCED FUNCTIONAL MATERIALS

CdS-Nanoparticle/Polymer Composite Shells Grown on Silica Nanospheres by Atom Transfer Radical Polymerization**

By *Tieyu Cui*, *Junhu Zhang*, *Jiayu Wang*, *Fang Cui*, *Wei Chen*, *Fubin Xu*, *Zheng Wang*, *Kai Zhang*, and *Bai Yang**

In this paper we describe the combined use of surface-initiated atom transfer radical polymerization (ATRP) and a gas/solid reaction in the direct preparation of CdS-nanoparticle/block-copolymer composite shells on silica nanospheres. The block copolymer, consisting of poly(cadmium dimethacrylate) (PCDMA) and poly(methyl methacrylate) (PMMA), is obtained by repeatedly performing the surface-initiated ATRP procedures in *N*,*N*-dimethylformamide (DMF) solution at room temperature, using cadmium dimethacrylate (CDMA) and methyl methacrylate (MMA) as the monomers. CdS nanoparticles with an average size of about 3 nm are generated in situ by exposing the silica nanospheres coated with block-copolymer shells to H_2S gas. These synthetic core–shell nanospheres were characterized using transmission electron microscopy (TEM), dynamic light scattering (DLS), thermogravimetric analysis (TGA), diffuse reflectance UV-vis spectroscopy, X-ray photoelectron spectroscopy (XPS), and powder X-ray diffraction (XRD). These composite nanospheres exhibit strong red photoluminescence in the solid state at room temperature.

1. Introduction

Core–shell nanospheres have attracted considerable attention in recent years due to their excellent optical, electrical, photoelectric, magnetic, and catalytic properties, together with the possibility for use as nanometer-scale building blocks to be assembled into periodic functional materials.[1–8] To date, various methods to synthesize core–shell nanospheres with different structures, sizes, and compositions have been employed, such as a colloid-reduction chemical method,[8] a sonochemical approach,[9] a sol–gel method,[10] homogeneous precipitation,[11] and a layer-by-layer-assembly method.[12,13] One of the most important challenges in this area is the controllable coating of nanospheres with organized polymer layers.[14–18] The polymer shell is intriguing for possible enhancement of the stability, wetting, dispersibility, and compatibility of the nanospheres.

Among many approaches to the surface coating of nanospheres with polymer layers, the surface-initiated atom transfer radical polymerization (ATRP) method has gained more and more attention recently.[19] Surface-initiated ATRP is a suitable method for the controllable preparation of polymer layers covalently bound to the surface of different solid materials, and even for the generation of block-copolymer grafts, because with this method it is easy to control the molecular weight, molecular-weight distribution, and composition of the block copolymer. Moreover, ATRP is compatible with a variety of functionalized monomers, thereby permitting the controllable synthesis of a broad range of polymers.[20–28] It has been used in many nanoparticle@polymer core–shell systems with different kinds of cores, such as SiO_2,[22,24] Au,[6,29] $MnFe_2O_4$,[30] and Fe_2O_3.[18]

Recently, we have reported a novel strategy for the controllable fabrication of nanoparticle/polymer composite thin films on planar substrates by combining surface-initiated ATRP and a gas/solid reaction.[31] In the present contribution, we extend this methodology to silica nanospheres for fabricating functional silica nanospheres with CdS-nanoparticle/block-copolymer composite shells. For the direct polymerization of cadmium dimethacrylate (CDMA)—a new metal-salt monomer containing two C=C bonds—the metal-containing monomer provides metal centers in the bound polymer chains for the further introduction of densely dispersed functional CdS nanoparticles into the composite shells. The crosslinked nanocomposite shells covalently bonded to the surface of inorganic silica cores will efficiently enhance the stability of core–shell nanospheres. Moreover, by controlling the ATRP process, nanoshells with different compositions and structures have been prepared on silica nanospheres.

2. Results and Discussion

2.1. Reaction Procedure

The preparation of crosslinked CdS-nanoparticle/block-copolymer composite shells on silica nanospheres involves several steps (Scheme 1). In the first step, an initiator monolayer for ATRP was modified on the surface of silica nanospheres by surface reaction with the Si–OH groups.[31] Subsequently, controllable surface-initiated polymerization of CDMA or methyl methacrylate (MMA) was performed on the initiator-modified

[*] Prof. B. Yang, T. Cui, Dr. J. Zhang, J. Wang, F. Cui, W. Chen, F. Xu, Z. Wang, K. Zhang
Key Lab for Supramolecular Structure & Materials
College of Chemistry, Jilin University
Changchun 130012 (P.R. China)
E-mail: byangchem@jlu.edu.cn

[**] This work was supported by the Special Funds for Major State Basic Research Projects (No. 2002CB613401) and the National Natural Science Foundation of China (No. 20374024, 200340062).

 DOI: 10.1002/adfm.200400327

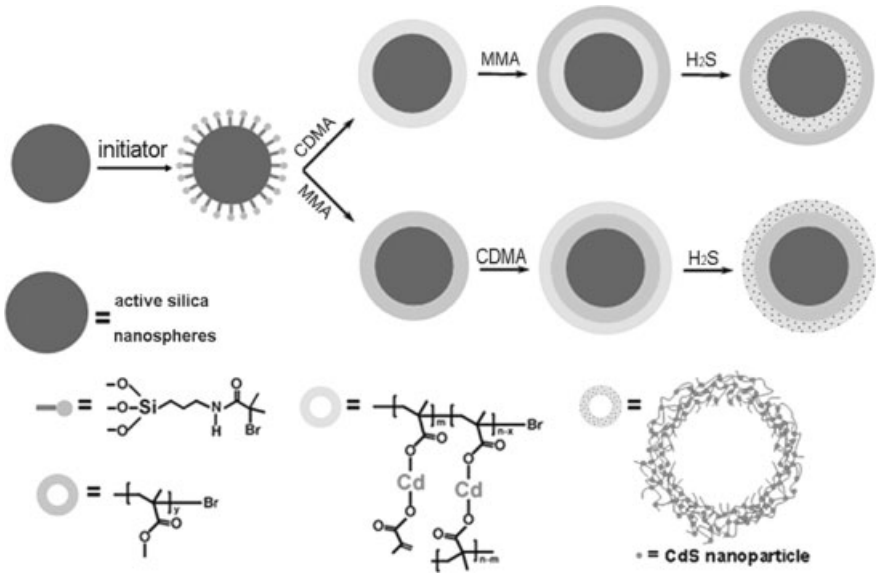

Scheme 1. Synthetic pathway for the preparation of silica nanospheres with CdS-nanoparticle/block-copolymer composite shells.

silica nanospheres in a polymerization bath containing monomer, catalyst, ligand, and solvent, with continuous stirring under a high-purity nitrogen stream at room temperature. Silica nanospheres with uniform polymer shells—SiO_2@PCDMA or SiO_2@PMMA—were formed. In the next step, on the basis of the first polymer shells, block copolymerizations were performed in the same manner as for typical surface-initiated ATRP procedures, producing silica nanospheres with uniform block-copolymer shells—SiO_2@PCDMA@PMMA or SiO_2-@PMMA@PCDMA. As we have reported recently,[31] since there are two C=C bonds in each CDMA molecule, a crosslinked PCDMA shell is produced in the above polymerization procedure, which enhances the mechanical strength and the thermal and chemical stability of the core–shell nanoparticles. Finally, CdS nanoparticles were generated in situ by exposing the SiO_2@PCDMA@PMMA or SiO_2@PMMA@PCDMA nanospheres to H_2S gas at 100 °C for 2 h.

2.2. Formation of Block-Copolymer Shells

The formation of the silica nanospheres with uniform block-copolymer shells was examined using transmission electron microscopy (TEM). Figure 1 shows the TEM images of a series of silica nanospheres coated with initiator monolayers (A) and different polymer shells (B–E). The initiator-grafted silica nanospheres have a smooth surface, and surface-initiated ATR (co)polymerization produces uniform homopolymer and diblock-copolymer shells

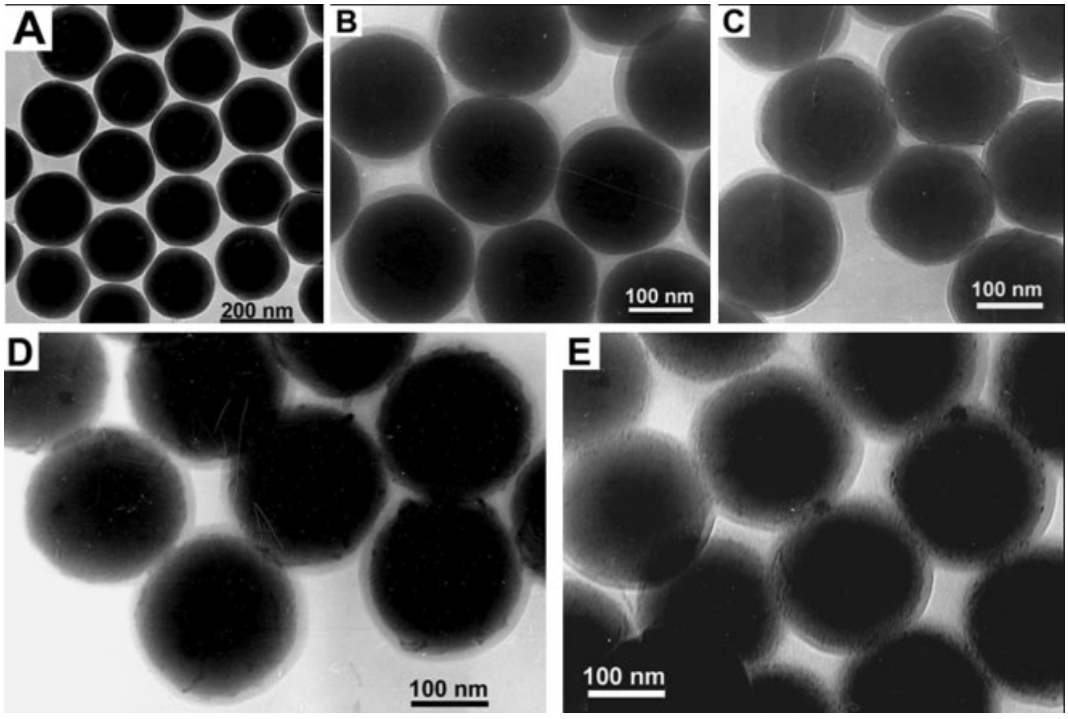

Figure 1. TEM images of initiator-coated SiO_2 nanospheres (A), SiO_2@PCDMA nanospheres (B), SiO_2@PMMA nanospheres (C), SiO_2@PCDMA@PMMA nanospheres (D), and SiO_2@PMMA@ PCDMA nanospheres (E).

ADVANCED FUNCTIONAL MATERIALS

on the surface of the silica nanospheres. The TEM images confirm the increase of the diameters from bare nanospheres (D_{SiO_2} = 206 nm) to homopolymer-coated silica nanospheres ($D_{SiO_2@PCDMA}$ = 215 nm and $D_{SiO_2@PMMA}$ = 219 nm) and to diblock-copolymer-coated silica nanospheres ($D_{SiO_2@PCDMA@PMMA}$ = 226 nm and $D_{SiO_2@PMMA@PCDMA}$ = 229 nm). Thermogravimetric analysis (TGA) data under a nitrogen-gas environment show that the proportion of organic components of the SiO_2@PCDMA@PMMA and SiO_2@PMMA@PCDMA nanospheres can reach as much as 20 % and 23 %, respectively. Furthermore, TEM and dynamic light-scattering (DLS) investigations reveal that the (co)polymer-coated silica nanospheres are still individual particles after the graft polymerization, and the size distribution of the (co)polymer-coated silica nanospheres is unaffected by the grafting process.

The thickness of the crosslinked nanocomposite shells depends on many parameters, including the monomer and catalyst concentrations, the polymerization time, and reaction temperature of the ATRP system, etc. We found that it was convenient and reproducible to control the thickness of the PCDMA shells by adjusting the concentration of the catalyst. The thickness of the PCDMA shells shows an almost linear increase with the concentration of CuCl catalyst (molar ratio $CuCl/CuBr_2/bpy = 10:3:30$ (bpy = 2,2′-bipyridine)) (Fig. 2); these data were obtained by allowing the surface-initiated polymerization of CDMA to proceed for the same period of time (24 h). When the concentration of CuCl increased to above 40 mmol L^{-1}, the rate of increase of the thickness became less, and when the concentration exceeded 50 mmol L^{-1} the catalysts and the ligand did not dissolve completely in our experimental conditions, so we were unable to obtain accurate data at higher concentrations. The diameters of the SiO_2@PCDMA nanoparticles were determined using DLS measurements in ethanol solution at 25 °C. The thickness of the PCDMA shells, in nanometers, was then calculated according to the formula

$$\text{Thickness of PCDMA shells} = (D_{SiO_2@PCDMA} - D_{SiO_2})/2 \quad (1)$$

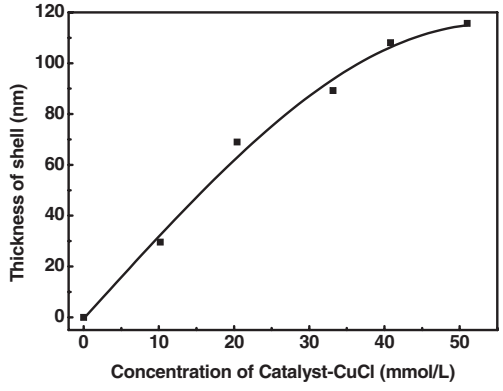

Figure 2. Plot of the PCDMA shell thickness versus concentration of CuCl catalyst.

2.3. CdS Nanoparticles in Block-Copolymer Shells

CdS nanoparticles were prepared in situ by exposing SiO_2@PCDMA@PMMA or SiO_2@PMMA@PCDMA nanospheres to H_2S gas at 100 °C for 2 h. The SiO_2@PCDMA@PMMA nanospheres gradually turned from white to brown–yellow (light yellow for the SiO_2@PMMA@PCDMA nanospheres). Figure 3 shows the typical diffuse reflectance UV-vis spectra (in Kubelka–Munk units) for SiO_2@PCDMA@PMMA and SiO_2@PMMA@PCDMA nanospheres after reaction with H_2S. It can be seen that an obvious absorption emerges in the visible region for these composite nanospheres, suggesting the formation of CdS nanoparticles.

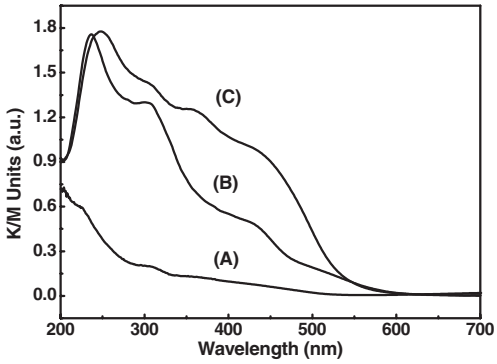

Figure 3. Diffuse-reflectance UV-Vis spectra for SiO_2@ PMMA@PCDMA nanospheres (A), SiO_2@PMMA@PCDMA nanospheres (B), and SiO_2@PCDMA@PMMA nanospheres (C) after reaction with H_2S at room temperature.

In order to confirm the formation of CdS nanoparticles and their crystallographic phase, X-ray photoelectron spectroscopy (XPS) and powder X-ray diffraction (XRD) data were recorded for SiO_2@PCDMA@PMMA and SiO_2@PMMA@PCDMA nanospheres after reaction with H_2S gas. The Cd and S peaks in the X-ray photoelectron spectra are observed at 405 and 161.5 eV, respectively, corresponding well with the expected values for Cd bound to sulfur. A half-quantitative analysis of these spectra gave an approximately equimolar ratio. The X-ray photoelectron spectra of Br indicate that there are still a large number of initiator Br atoms on the surfaces of the SiO_2@PCDMA@PMMA and SiO_2@PMMA@PCDMA nanospheres before and after reaction with H_2S (Fig. 4). The diffuse, broad diffraction patterns of bare silica nanospheres and SiO_2@PCDMA@PMMA and SiO_2@PMMA@PCDMA nanospheres after reaction with H_2S gas are shown in Figure 5. It can be seen from this figure that the powder XRD patterns of bare silica nanospheres show only one broad diffraction peak at around 23.0°, whereas the powder XRD diffraction patterns of the composite nanospheres contain three strong diffraction peaks at 26.5°, 44.2°, and 52.2°, which is consistent with the major peaks previously reported for hexagonal CdS. The peak at 26.5° was deconvoluted into three peaks, at 24.8° (100), 26.5° (002), and 28.2° (101).[32] The average sizes of the CdS nano-

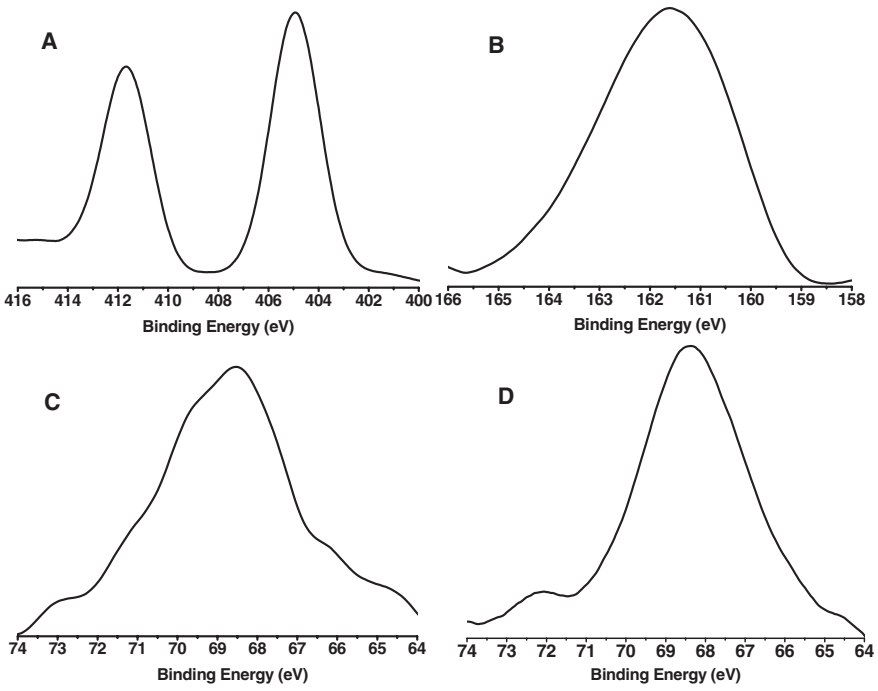

Figure 4. Cd (A) and S (B) XPS spectra of SiO_2@PMMA@PCDMA nanospheres. Br XPS spectra of SiO_2@PMMA@PCDMA nanospheres before (C) and after (D) reaction with H_2S.

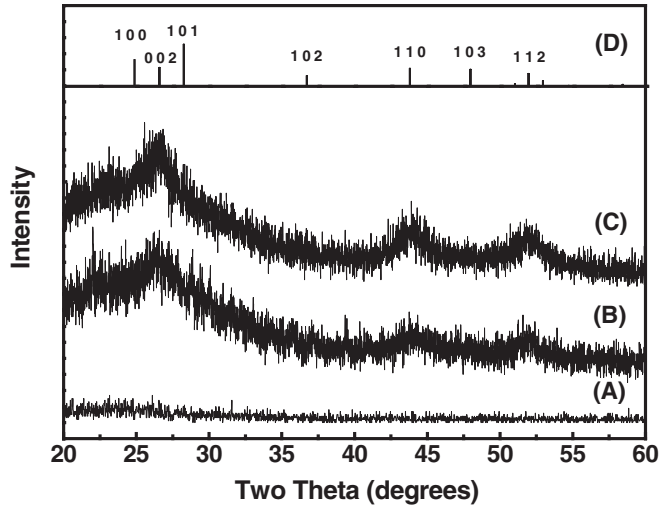

Figure 5. Powder XRD patterns for initiator-coated SiO_2 nanospheres (A), SiO_2@PCDMA@PMMA nanospheres (B), SiO_2@PMMA@PCDMA nanospheres after reaction with H_2S (C), and CdS bulk crystals (D).

particles in SiO_2@PCDMA@PMMA and SiO_2@PMMA@PCDMA nanospheres after reaction with H_2S gas are about 3.0 nm and 3.5 nm, respectively, as calculated from the Scherrer equation.[32,33]

Figure 6A shows the TEM image of SiO_2@PCDMA@PMMA nanospheres after reaction with H_2S. CdS nanoparticles can be seen between the SiO_2 cores and the PMMA shells. The CdS nanoparticles in the nanocomposite could be extracted by adding *n*-hexadecyl mercaptan to a nanocomposite/*N*,*N*-dimethylformamide (DMF) suspension and sonicating the mixture for 20 min. The mercapto groups bind to the Cd^{2+} at the surface of the CdS nanoparticles, replacing the carboxy groups, and then the CdS nanoparticles are extracted from the composite shells into the *n*-hexadecyl mercaptan phase. The TEM image and the selected-area electron diffraction (SAED) pattern of the CdS nanoparticles extracted into the *n*-hexadecyl mercaptan phase are shown in Figure 6B. We can clearly see that the CdS nanoparticles are uniform with a diameter of about 3 nm, in good agreement with the results above. The SAED pattern also confirms the crystal structure of the hexagonal CdS nanoparticles.

The SiO_2@PCDMA@PMMA and SiO_2@PMMA@PCDMA nanospheres show strong photoluminescence in the solid state at room temperature after reaction with H_2S gas (Fig. 7). The intense emissions of SiO_2@PCDMA@PMMA and SiO_2@PMMA@PCDMA nanospheres, centered at 617 nm and 604 nm ($\lambda_{ex} = 453$ nm), respectively, are not present in the corresponding spectra of SiO_2-only nanospheres, but match the emission maximum of the CdS nanoparticles. A similar emission band close to 610 nm has also been observed previously for CdS nanoparticles incorporated into polymers.[33–35] The photoluminescence spectra of CdS nanoparticles in the polymer shells prepared by the present method are dominated by defect emissions.[34] The most common defects present in these small CdS nanoparticles are sulfur vacancies, which give rise to the characteristic red luminescence.

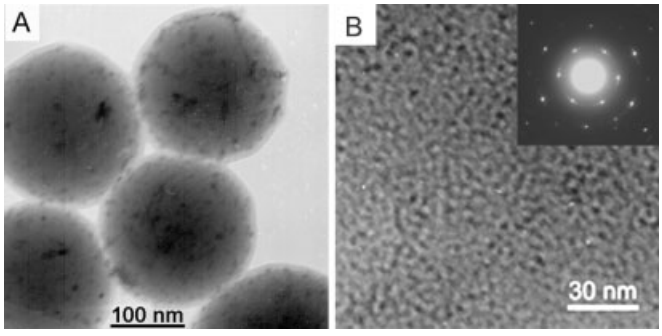

Figure 6. TEM images of SiO_2@PCDMA@PMMA nanospheres after reaction with H_2S (A), and CdS nanoparticles extracted from these nanospheres (B); inset: SAED pattern of the same CdS nanoparticles.

ADVANCED FUNCTIONAL MATERIALS

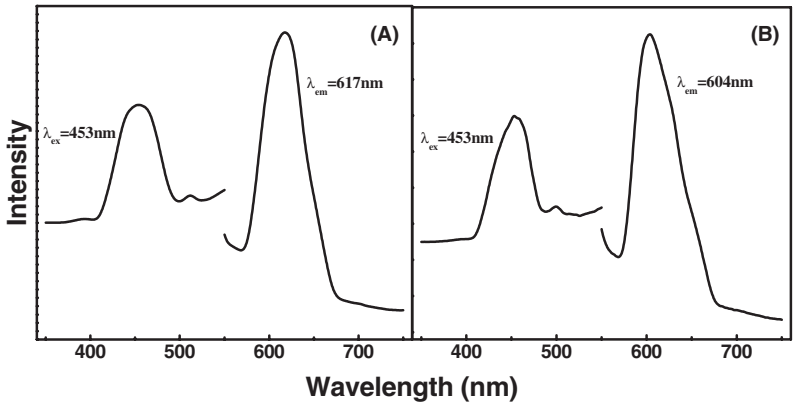

Figure 7. Solid-state photoluminescence spectra of SiO_2@PCDMA@PMMA nanospheres (A) and SiO_2@ PMMA@PCDMA nanospheres (B) after reaction with H_2S at 100 °C for 2 h.

3. Conclusions

We have demonstrated a practical route for the direct synthesis of silica nanospheres with CdS-nanoparticle/block-copolymer composite shells by combining surface-initiated ATRP and a gas/solid reaction. This procedure should be extendable to many other systems that involve the use of different functional metal-containing monomers to fabricate triblock-copolymer nanocomposites. The XPS results indicate that there are still a large number of initiator Br atoms on the surfaces of the SiO_2@PCDMA@PMMA and SiO_2@PMMA@PCDMA nanospheres before and after reaction with H_2S. This should open up a wider route to promote the fabrication of new types of materials on which multiple functional groups can be concentrated.

4. Experimental

Materials: Methyl methacrylate (MMA, 99.5 %) was distilled from powdered KOH under vacuum and stored at –15 °C before use. Dichloromethane and toluene were distilled over dried zeolite (4 Å). (3-Aminopropyl)triethoxysilane (99 %), 2-bromo-2-methylpropionic acid (98 %), 1,3-dicyclohexylcarbodiimide (DCC, 1.0 M solution in dichloromethane), copper(II) bromide (99.999 %), and 2,2′-bipyridine (bpy, 99+ %) were purchased from Aldrich and used without further purification. Copper(II) chloride (99.99 %, Acros) was stored under a high-purity nitrogen (99.999 %) atmosphere. *n*-Hexadecyl mercaptan (92+ %, Acros), 4-(dimethylamino)pyridine (DMAP, 99 %, Fluka), *N*,*N*-dimethylformamide (DMF), CdO, methacrylic acid (MA), hydrogen peroxide, and concentrated sulfuric acid were used as received.

Synthesis of CDMA: CdO (64.2 g) was added to a 500 mL three-necked flask containing MA (90 mL) and distilled water (120 mL). The reaction mixture was stirred continuously for at least 1.5 h at 60 °C to dissolve the CdO powder entirely. After filtration, the filtrate was vacuum distilled to remove some of the water and the unreacted MA, and then the remainder was cooled to separate out the white powder of cadmium dimethacrylate (CDMA). The powder was collected by filtration and recrystallized from ethanol to give white flaky crystals. Finally, the resulting white crystals were dried in a vacuum oven at room temperature for 24 h.

Pretreatment of Silica Nanospheres: Silica nanospheres were prepared in ethanol according to the Stöber method [36–38] at ambient temperature. The silica nanospheres were re-suspended by sonication in a mixed solution of concentrated sulfuric acid and hydrogen peroxide with an H_2SO_4/H_2O_2 volume ratio of 7:3. The suspension of silica nanospheres was heated at 90 °C for 24 h. After surface activation, these nanospheres were washed by ultrasonic re-suspension (in distilled water)/centrifugation cycles to neutrality. The white precipitate was dried in a vacuum oven at room temperature overnight to give a white granular powder.

Growth of Initiator Monolayer: The silica nanospheres (2.26 g) and dry toluene (18.1 mL) were added to a 50 mL conical flask containing a magnetic stirrer bar. The flask was fitted with a rubber plug and sonicated for 10 min. (3-Aminopropyl)triethoxysilane (0.9 mL) was then added to the flask with a syringe, and the mixture stirred at room temperature for 24 h. The silica nanospheres were then washed in succession, with centrifugation and ultrasonic re-suspension, with dry toluene, acetone, toluene, acetone, and absolute ethanol, and then all volatile materials were removed under vacuum. The amino-grafted silica nanospheres (2.12 g) were re-suspended in a mixed solution of 2-bromo-2-methylpropionic acid (590 mg), DMAP (106 mg), and dry methylene chloride (177 mL). The suspension was cooled to 0 °C, and then 4.4 mL of DCC was added. The suspension was stirred at room temperature for 24 h. The initiator-grafted silica nanospheres were washed successively, with centrifugation and ultrasonic re-suspension, with dry methylene chloride, toluene, acetone, and absolute ethanol. Finally, all volatile materials were removed under vacuum.

Surface-Initiated ATRP of CDMA: The initiator-modified silica nanospheres (300 mg) were re-suspended in 10 mL of a DMF solution of CDMA (4.200 g) in a flask. High-purity nitrogen (99.999 %) was bubbled through this mixture for 30 min. CuCl, $CuBr_2$, and bpy (CuCl/$CuBr_2$/bpy = 10:3:30, molar ratio) were added with continuous stirring; the dispersion became dark brown. The reaction was performed under a high-purity nitrogen atmosphere and allowed to proceed at room temperature for 24 h. The polymerization reaction was terminated by pouring the reaction solution into a large amount of alcohol in air. The color of the solution became blue, and the nanoparticles were then washed with several cycles of centrifugation and re-suspension until they became white. Finally, the resulting white powder was dried in a vacuum oven at 40 °C overnight (NB: different concentrations of CuCl in the system give different shell thicknesses of the nanocomposite).

Surface-Initiated ATRP of CDMA and MMA: The initiator-modified silica nanospheres (250 mg) were re-suspended in 10 mL of a DMF solution of CDMA (1.843 g) or MMA (6 mL) in a flask. High-purity nitrogen (99.999 %) was bubbled through this mixture for 30 min. CuCl (5.1 mg), $CuBr_2$ (3.4 mg), and bpy (22.6 mg) were then added with continuous stirring. The reaction was performed under a high-purity nitrogen atmosphere and allowed to proceed at room temperature for 24 h. Then, the reaction solution was poured into a large amount of ethanol in air to terminate the polymerization reaction. The solution became blue for a few hours. The nanospheres were then washed with several cycles of centrifugation and re-suspension until they became white. The copolymerization reactions of the PCDMA-coated silica nanospheres (207 mg), MMA (6 mL), CuCl (5.1 mg), $CuBr_2$ (3.3 mg), and bpy (24.3 mg), as well as the PMMA-coated silica nanospheres (287 mg), MMA (6 mL), CuCl (5.1 mg), $CuBr_2$ (3.2 mg), and bpy (24.7 mg) were performed under the same conditions. The silica nanospheres with block-copolymer shells were then put into an evacuated vial and an excess of H_2S gas was injected into it. The reaction was carried out for 2 h at 100 °C to enable the Cd ions to be converted entirely into CdS nanoparticles.

Analysis: TEM images were obtained with a Hitachi H 8100 TEM. XPS spectra were measured with a VG Escalab MK II spectrometer with a monochromatic Mg Kα X-ray source (E_{exc} = 1256.3 eV). All binding energies were referenced by setting the CH_x peak maximum in

ADVANCED FUNCTIONAL MATERIALS

the C_{1s} spectrum to 284.6 eV. ^{1}H NMR spectra were recorded in $(CD_3)_2SO$ using a Bruker AV400 400 MHz spectrometer. TGA were performed on a Netzsch STA 449C thermogravimetric analyzer under a nitrogen gas environment at a heating rate of 20 °C min^{-1}. The diffuse-reflectance UV-vis spectra were recorded using a Perkin–Elmer Lambda 20 UV-Vis spectrometer. The photoluminescent spectra were obtained on a Perkin–Elmer LS55 luminescence spectrometer. Powder XRD data were collected on a Siemens D5005 diffractometer with Cu Kα radiation ($\lambda = 1.5418$ Å). DLS analysis was performed at 25 °C with a Malvern Zetasizer 3000 HSA at a fixed scanning angle of 90°.

Received: July 21, 2004
Final version: August 12, 2004

[1] W. B. Russell *Nature* **2003**, *421*, 490.
[2] C. H. M. Hofman-Caris, *New J. Chem.* **1994**, *18*, 1087.
[3] F. Caruso, *Adv. Mater.* **2001**, *13*, 11.
[4] G. Kickelbick, D. Holzinger, C. Brick, G. Trimmel, E. Moons, *Chem. Mater.* **2002**, *14*, 4382.
[5] W. Guo, J. J. Li, Y. A. Wang, X. Peng, *J. Am. Chem. Soc.* **2003**, *125*, 3901.
[6] K. Kamata, Y. Lu, Y. Xia, *J. Am. Chem. Soc.* **2003**, *125*, 2384.
[7] X. Teng, D. Black, N. J. Watkins, Y. Gao, H. Yang, *Nano Lett.* **2003**, *3*, 261.
[8] S. W. Kim, M. Kim, W. Y. Lee, T. Hyeon, *J. Am. Chem. Soc.* **2002**, *124*, 7642.
[9] V. G. Pol, A. Gedanken, J. Calderon-Moreno, *Chem. Mater.* **2003**, *15*, 1111.
[10] M. M. Y. Chen, A. Katz, *Langmuir* **2002**, *18*, 8566.
[11] K. P. Velikov, A. van Blaaderen, *Langmuir* **2001**, *17*, 4779.
[12] F. Caruso, M. Spasova, V. Salgueirino-Maceira, L. M. Liz-Marzán, *Adv. Mater.* **2001**, *13*, 1090.
[13] D. Wang, A. L. Rogach, F. Caruso, *Chem. Mater.* **2003**, *15*, 2724.
[14] K. J. Watson, J. Zhu, S. T. Nguyen, C. A. Mirkin, *J. Am. Chem. Soc.* **1999**, *121*, 462.
[15] D. Gan, L. A. Lyon, *J. Am. Chem. Soc.* **2001**, *123*, 7511.
[16] C. R. Vestal, Z. J. Zhang, *J. Am. Chem. Soc.* **2002**, *124*, 14312.
[17] J. Zhang, N. Coombs, E. Kumacheva, *J. Am. Chem. Soc.* **2002**, *124*, 14 512.
[18] Y. Wang, X. Teng, J. S. Wang, H. Yang, *Nano Lett.* **2003**, *3*, 789.
[19] G. Li, J. Fan, R. Jiang, Y. Gao, *Chem. Mater.* **2004**, *16*, 1835.
[20] K. Matyjaszewski, J. Xia, *Chem. Rev.* **2001**, *101*, 2921.
[21] T. E. Patten, K. Matyjaszewski, *Adv. Mater.* **1998**, *10*, 901.
[22] J. Pyun, K. Matyjaszewski, *Chem. Mater.* **2001**, *13*, 3436.
[23] T. von Werne, T. E. Patten, *J. Am. Chem. Soc.* **1999**, *121*, 7409.
[24] T. von Werne, T. E. Patten, *J. Am. Chem. Soc.* **2001**, *123*, 7497.
[25] J. Pyun, K. Matyjaszewski, T. Kowalewski, D. Savin, G. Patterson, G. Kickelbick, N. Huesing, *J. Am. Chem. Soc.* **2001**, *123*, 9445.
[26] S. Nuß, H. Böttcher, H. Wurm, M. Hallensleben, *Angew. Chem. Int. Ed.* **2001**, *40*, 4016.
[27] D. Bontempo, N. Tirelli, K. Feldman, G. Masci, V. Crescenzi, J. A. Hubbell, *Adv. Mater.* **2002**, *14*, 1239.
[28] B. Gu, A. Sen, *Macromolecules* **2002**, *35*, 8913.
[29] T. K. Mandal, M. S. Fleming, D. R. Walt, *Nano Lett.* **2002**, *2*, 3.
[30] C. R. Vestal, Z. J. Zhang, *J. Am. Chem. Soc.* **2002**, *124*, 14312.
[31] J. Y. Wang, W. Chen, A. H. Liu, G. Lu, G. Zhang, J. H. Zhang, B. Yang, *J. Am. Chem. Soc.* **2002**, *124*, 13 358.
[32] M. E. Wankhede, S. K. Haram, *Chem. Mater.* **2003**, *15*, 1296.
[33] E. F. Hilinski, P. A. Lucas, *J. Chem. Phys.* **1988**, *89*, 3435.
[34] S. C. Farmer, T. E. Patten, *Chem. Mater.* **2001**, *13*, 3920.
[35] J. Zhang, N. Coombs, E. Kumacheva, Y. Lin, E. H. Sargent, *Adv. Mater.* **2002**, *14*, 1756.
[36] W. Stöber, A. Fink, *J. Colloid Interface Sci.* **1968**, *26*, 62.
[37] A. P. Philipse, A. J. Vrij, *J. Colloid Interface Sci.* **1989**, *128*, 121.
[38] G. H. Bogush, M. A. Tracy, C. F. Zukowski IV, *J. Noncryst. Solids* **1988**, *104*, 95.

